Determination of the Sky Projected Spin-Orbit Angle using Radial Velocity data for WASP-16, WASP-25, and WASP-31 systems

Enlightened Anteaters
University of Rochester, Department of Physics and Astronomy, Rochester, New York
(Dated: March 25, 2025)

It is believed that "hot Jupiters", large gas giants that live within a fraction of an AU from their host star, did not form at their present location but were driven there via some sort of migration mechanism. Measurements of the spin orbit alignment angle may provide a method to distinguish between two competing migration theories, the disk migration model and the Kozai-Lidov model. In this paper, the sky projected spin orbit angles for WASP-16, WASP-25, and WASP-31 planetary systems are determined using measurements of the Rossiter-McLaughlin effect where Markov Chain Monte Carlo (MCMC) is used to probe the parameter space.

I. INTRODUCTION

A. Hot Jupiters

The search for planets outside our solar system, or *exoplanets*, has blossomed into an active field of research ever since the discovery of the first exoplanet in 1995 by Michel Mayor & Didier Queloz [1]. Since then, more than 5,000 exoplanets have been discovered. Before the discovery of exoplanets, our knowledge of planet formation was based only on what we could observe in the solar system. The standard theory of planetary formation is that planets form from a cloud of gas and dust that collapses into a disk. Beyond a certain distance from the host star, called the *snow line*, the gas is cold enough that solid icy materials are abundant, allowing for the rapid development of large rocky cores with gaseous atmospheres [2]. Within the snow line, solid material is sparse, and so rocky cores are not large enough to attract gas, growing instead via massive collisions with other objects [2]. From this "solar-centric" model, we expect that terrestrial planets should orbit close to the host star, followed by gas giants [2].

In 1995, the discovery by Mayor and Queloz of a so called "hot Jupiter", 51 Pegasi b, immediately challenged the solar-centric model of planetary formation [2], [3]. Orbiting around a sun like star, 51 Pegasi b is a Jupiter mass planet with an orbital period of a mere *four days*. Moreover, it is *ten times* closer to the host star than Mercury is to the sun, clearly well inside the snow line. The existence of such a planet was not an anomaly, with more hot Jupiters discovered in 1997 by Butler [2].

At present, it is believed that hot Jupiters do not form at their present location *in situ*, but instead have their orbits altered by some sort of migration mechanism that brings them from beyond the snow line to within a fraction of an astronomical unit of the host star [2]. The theory of disk migration for Jupiter sized planets, Type II migration, posits that a hot Jupiter forms from a circumstellar disk at a reasonable distance of several AU from the host star before following the material of the disk as it moves towards the star [4]. Another possible mechanism is the Kozai-Lidov effect, where the presence of a third body perturbs the motion of the planet. This creates oscillations in both the eccentricity and inclination of the orbit, leading to inward migration [5].

The *sky projected spin-orbit alignment angle* λ, the angle between the stellar rotation axis and the planet's orbital plane, of hot Jupiter systems can help determine which mechanism is responsible for the location of hot Jupiters. The disk migration model predicts that hot Jupiter systems should be well aligned, whereas the Kozai-Lidov mechanism should produce a continuum of inclinations, and so hot Jupiters should have misaligned orbits [5]. Orbits are considered misaligned if $|\lambda| \geq 0°$ at $> 3\sigma$ significance or $|\lambda| \geq 30°$ [6]. The sky-projected spin-orbit alignment angle can be determined by measuring the *Rossiter-McLaughlin effect*; however, determination of the *true* spin-orbit alignment angle ψ is nontrivial. Triaud et al. (2010) [5] generated a distribution of (ψ) from the measurement of individual planets assuming that stellar rotation axes are randomly oriented on the sky. Their findings matched the theoretical distribution of Fabrycky & Tremaine (2007) [7] for Kozai–Lidov mechanism dominated migration, implying that disk migration might not be a significant criteria for explaining the occurrence of hot Jupiters.

In this paper, we will estimate the sky-projected spin orbit angle λ for a hot Jupiter by fitting measurements of the Rossiter-McLaughlin effect with the analytical model derived by Ohta et al. (2005) [8] via both maximization of a log likelihood and Markov Chain Monte Carlo.

II. MODEL

A. The Rossiter-McLaughlin Effect

Due to the presence of the hot Jupiter, the host star does not remain completely stationary; it orbits the common center of mass. When the star moves towards an observer, we observe that spectral lines broaden towards smaller wavelengths (blueshift), and when it moves away lines broaden towards larger wavelengths (redshift) [9]. The radial velocity of the star can be determined by measuring this Doppler broadening. When the Jupiter transits its host star, it blocks off the light coming from

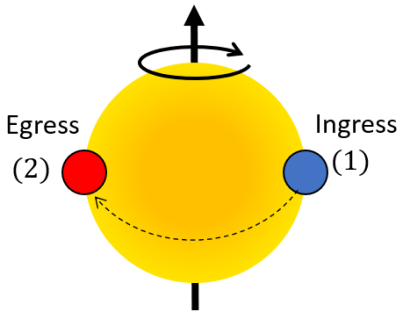

FIG. 1. A planet transiting its host star, creating the Rossiter-McLaughlin effect. At position (1), the planet blocks blueshifted light so spectral lines broaden only on the long wavelength side. The opposite effect with redshifted light occurs at position (2). Graphic adapted from Gaudi & Winn (2007) [9].

the different parts of the stellar disk in a time dependent manner, as shown in Figure 1. This causes an asymmetric distortion of the spectral lines of a star due to its spin leading to an apparent anomaly in the line-of-sight radial velocities, known as the Rossiter–McLaughlin Effect (RM Effect) [10], [11]. Figure 2 shows theoretical radial velocity curves for a star with an exoplanet. Ordinarily, the curve is sinusoidal, but a transiting planet creates an additional waveform: the RM anomaly.

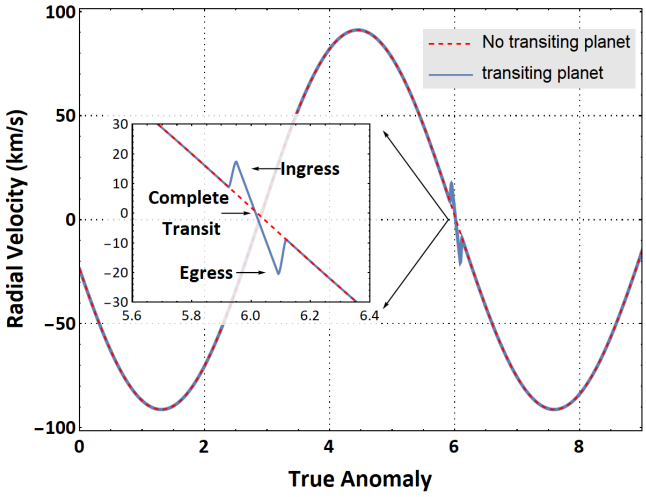

FIG. 2. The dashed red line is a theoretical model for the observed radial velocity curve due to the host star orbiting the common center of mass. However, when the planet transits, the RM anomaly can be seen (blue curve).

Measurements of the RM effect can be used to determine the sky-projected spin-orbit alignment angle. To see this, we write the total radial velocity curve as

$$v_T = v_O + \Delta v_{RM}(\lambda) \tag{1}$$

where v_O is the radial velocity in the *absence* of a transiting exoplanet due to orbital motion and $\Delta v_{RM}(\lambda)$ is the change in the observed radial velocity due to the RM effect, which is dependent on λ.

Ohta et al. (2005) [8] derives analytical expressions for v_O and Δv_{RM}. These equations depend on many parameters, and for the sake of brevity are presented here without an in-depth explanation. The contribution from orbital motion (as a function of true anomaly f) is

$$v_O = V_{SV} - \frac{m_p}{m_p + m_s}\frac{na\sin(i)}{\sqrt{1-e^2}}[\sin(f+\varpi) + e\sin\varpi] \tag{2}$$

where V_{SV} is the systematic velocity of the system, m_p, m_s are the masses of the planet and star respectively, n is the mean motion, a is the semi-major axis, i is the inclination angle of the orbit, ϖ is the negative longitude of the line of site, and e is the eccentricity of planetary orbit. Orbital motion must be accounted for while measuring the RM effect since it adds a time-varying offset to the data. The change due to the RM effect is broken into a complete transit phase, where the planet fully overlaps the star, and ingress and egress phases where the planet partially overlaps the star (Figure 1).

$$\Delta v_{RM} = \begin{cases} \Delta v_T & \text{Complete Transit Phase} \\ \Delta v_I & \text{Ingress and Egress Phase} \end{cases} \tag{3}$$

These contributions to the RM anomaly are given by

$$\Delta v_T = \frac{V\sin I_s}{R_s} X_p(\lambda)\frac{\gamma^2[1-\epsilon(1-W_2)]}{1-\gamma^2-\epsilon[1/3-\gamma^2(1-W_1)]} \tag{4}$$

and

$$\Delta v_I = \frac{V\sin I_s}{R_s} X_p(\lambda)\times \frac{(1-\epsilon)[-z_0\zeta + \gamma^2\cos^{-1}(\zeta/\gamma)] + [\epsilon/(1+\eta_p)]W_4}{\pi[1-(1/3)\epsilon] - (1-\epsilon)[\sin^{-1}z_0 - (1+\eta_p)z_0 + \gamma^2\cos^{-1}(\zeta/\gamma)] - \epsilon W_3} \tag{5}$$

where V is the rotational velocity of the star, X_p is the position of the planet, I_s is the inclination between stellar spin axis and the observer, γ is the ratio of planet radius to stellar radius, and ϵ is a limb darkening parameter. The parameters ζ, z_0 and η_p depend on the motion of the planet, while the W parameters result from integration of the stellar intensity profile. The dependence on λ enters through the parameters that depend on the motion of the planet.

It is obvious that this model, which accounts for linear stellar limb darkening, is complicated. The main takeaway for the reader should be that the RM effect depends on the sky projected spin orbit angle λ, and that many of the obscure parameters in the preceding equations are themselves functions of more recognizable quantities such as the star's radius and intensity profile, as well as the planet's radius and orbital radius.

III. DATA AND METHODS

Radial velocity data for three systems from the Wide Angle Search for transiting Planets, WASP-16, WASP-

System	References		Parameters					
			$R_s(R_\odot)$	a/R_s	γ	Period (Days)	ϵ	i
WASP-16	Brown et al. 2012	Southworth et al. 2013	1.08	8.20	0.110	3.12	0.9	85.22°
WASP-25	Brown et al. 2012	Southworth et al. 2014	0.92	11.1	0.133	3.76	0.64	88.0°
WASP-31	Brown et al. 2012	Bonomo et al. 2017	1.25	8.01	0.127	3.41	0.9	84.54°

TABLE I. We chose $V \sin I_s$ and λ as free parameters in a maximum likelihood estimate, while other parameters were set to the literature values shown above. Parameter values were obtained using Brown et al. 2012 [6] and the NASA exoplanet archive.

25, and WASP-31, was obtained from the data sets given in Brown et al. 2012 [6], who measured the RM effect using the HARPS high-precision echelle spectrograph.

First, we examined only the contribution to the radial velocity caused by the orbital motion of the star v_O, shown as the red dashed curve in Figure 2, in order to isolate the RM effect. This was performed first using a maximum likelihood estimation, where the likelihood was constructed assuming each data point was an independent measurement with Gaussian uncertainty. Later, a determination of parameters using MCMC was performed, where the posterior PDF was constructed using the likelihood as well as several Bayesian priors. Note that we have fit a scatter parameter $\mathfrak{N}$ which accounts for global data errors not reflected in the reported uncertainties (see Figure 6). There can be multiple reasons for the presence of this uncertainty component [12]. For example, this could be the result of another planet in the system or caused by the intrinsic anomalies in the star spectrum due to the irregularities on the surface of the star [13]. The priors were chosen in such a way that they should convey the known physical aspects of the system unambiguously. We used a flat prior on most parameters, and a Jeffreys Prior on the scale factors: orbital period (P), semi-amplitude (K) and $\mathfrak{N}$.

Although this fit contained no information about λ, the RM anomaly Δv_{RM} could now be isolated by determining the fit residuals. Once isolated, another maximum likelihood estimation was performed to fit the RM anomaly to equation (3), once again assuming that the data points were independent with Gaussian uncertainties. We chose λ and $V \sin I_s$ as fit parameters, while planetary and stellar information such as radius, orbital period, etc. were fixed at literature values found using the NASA exoplanet archive (see Table I). The fits are displayed in Figure 3, and the results Table II.

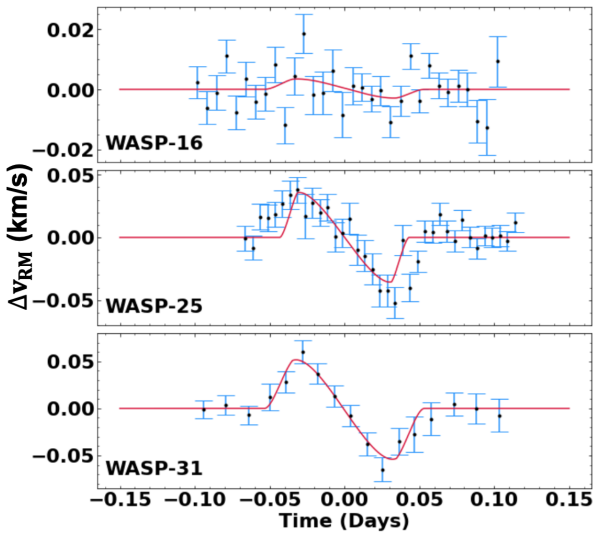

FIG. 3. Result of maximum likelihood fit of equation (3) to the RM anomaly. The anomaly was determined using the fit residuals from the first ML fit of equation (2).

System	λ (deg)	$V \sin I_s (km/s)$
WASP-16	-3.96 ± 26.30	0.64 ± 0.59
WASP-25	-0.20 ± 9.68	3.01 ± 0.43
WASP-31	1.05 ± 3.27	10.58 ± 1.67

TABLE II. Values of λ and $V \sin I_s$ obtained using Maximum Likelihood estimations. Due to poor convergence and large fit uncertainties, we then moved towards using Markov Chain Monte Carlo to explore the parameter space.

A. Markov Chain Monte Carlo

We quickly determined that not only did the result from ML estimations come with large errors, but any attempt to increase the amount of free parameters in our ML estimations led to poor convergence. We thus implemented an alternative methodology wherein the entire parameter space of equations (2) and (3) was explored with an Affine Invariant Markov Chain Monte Carlo Ensemble sampler. A swarm of best fit curves created using each MCMC walker trajectory is shown in Figure 4.

IV. RESULTS OF MCMC

As mentioned briefly in the preceding section, a determination of parameters using MCMC was performed on only the contribution to the radial motion caused by the orbital motion of the star. While these results are of

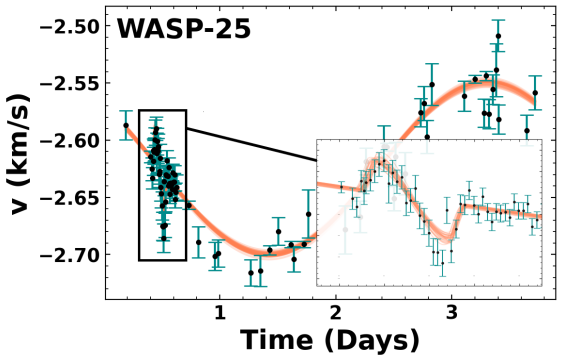

FIG. 4. A randomly chosen selection of MCMC parameter fits for WASP-25 data. The RM region is highlighted in the inset figure.

interest, the main purpose of this determination of parameters was for use in isolating the RM effect. In the interest of space, we have designated the results corresponding to parameters in equation (2) to the appendix where a corner plot showing the best fit values and uncertainties is provided. The fit from equation (2) was used only to determine the residuals which contain the RM effect.

Unlike those obtained from a pure maximum likelihood estimation, the parameters from our approach utilizing MCMC converged well for the RM anomaly. Figure 5 displays the posterior distributions from the Markov Chain Monte Carlo results for λ and $V \sin I_s$ for WASP-25 b. We chose to display these two parameters in particular because they can only be found from the RM effect and can be used to find the true spin orbit alignment angle ψ.

We find that the sky projected spin orbit angle for WASP-25 b, $\lambda = 18.60°$ is larger than the result in Brown et al. (2012) [6] but is ultimately consistent within uncertainty. Despite the larger angle, WASP-25 b still does not satisfy the criteria for being classified as misaligned. The two main criteria used to determine if a planet is misaligned are $|\lambda| \geq 0°$ at $> 3\sigma$ significance or $|\lambda| \geq 30°$ [6].

V. CONCLUSIONS

Determination of the spin orbit alignment angle provides evidence for either the disc migration model or Kozai-Lidov model as competing theories of planetary migration. We have determined orbital parameters as well as the sky projected spin orbit angle for WASP-25 b. First, our work demonstrates the power of Markov Chain Monte Carlo as a tool to determine orbital parameters of exoplanet systems when traditional minimizers are inadequate. Furthermore, our determination of the spin orbit alignment angle of WASP-25 suggests, based off commonly used criteria, that this planet is aligned, offering support to the result found by Brown et al. (2012). We caution that determining the alignment of a single planet is insufficient when deciding what model of planetary migration is most likely. Such a study would require an analysis of the current ensemble of hot Jupiter spin orbit alignment angle measurements. As more and more hot Jupiters are discovered, it would be interesting to apply our MCMC method to determine their spin orbit angles and classify their alignments. A future work could determine the true spin orbit angle ψ from the distribution of λ and compare to theoretical distribution that is predicted to occur due to the Kozai-Lidov mechanism [7].

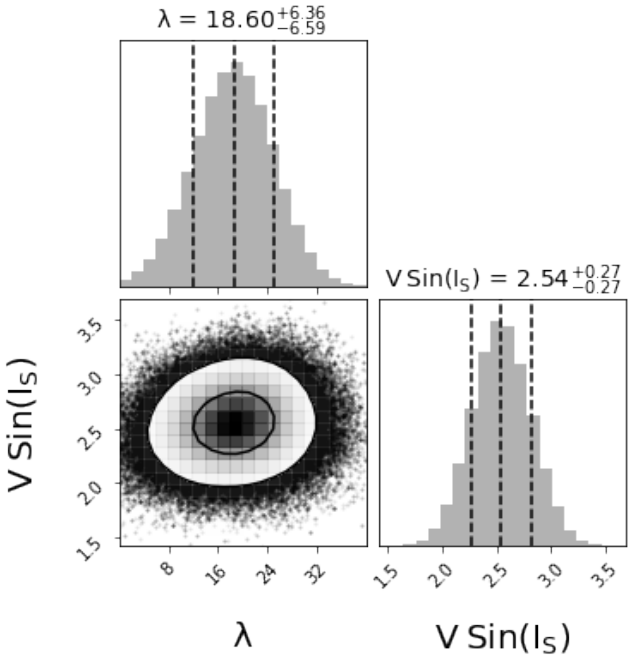

FIG. 5. Correlation of V sin(I$_S$) with λ for WASP-25 b. λ is greater than zero at 2 sigma significance, but not the 3 sigma significance required to classify the planet as misaligned.

VI. ACKNOWLEDGEMENTS

This paper makes use of data from the first public release of the WASP data (Butters et al. 2010) as provided by the WASP consortium and services at the NASA Exoplanet Archive, which is operated by the California Institute of Technology, under contract with the National Aeronautics and Space Administration under the Exoplanet Exploration Program. The authors would also like to thank Prof. Segev BenZvi (Univ. of Rochester) for the helpful suggestions.

[1] M. Mayor and D. Queloz, A Jupiter-mass companion to a solar-type star, Nature (London) **378**, 355 (1995).

[2] R. I. Dawson and J. A. Johnson, Origins of hot jupiters, Annual Review of Astronomy and Astrophysics **56**, 175 (2018).

[3] J. J. Fortney, R. I. Dawson, and T. D. Komacek, Hot jupiters: Origins, structure, atmospheres, Journal of Geophysical Research: Planets **126**, 10.1029/2020je006629 (2021).

[4] D. N. C. Lin, P. Bodenheimer, and D. C. Richardson, Orbital migration of the planetary companion of 51 pegasi to its present location, Nature **380**, 606 (1996).

[5] Triaud, A. H. M. J., Collier Cameron, A., Queloz, D., Anderson, D. R., Gillon, M., Hebb, L., Hellier, C., Loeillet, B., Maxted, P. F. L., Mayor, M., Pepe, F., Pollacco, D., Ségransan, D., Smalley, B., Udry, S., West, R. G., and Wheatley, P. J., Spin-orbit angle measurements for six southern transiting planets - New insights into the dynamical origins of hot Jupiters, Astronomy & Astrophysics **524**, A25 (2010).

[6] D. J. A. Brown, A. C. Cameron, D. R. Anderson, B. Enoch, C. Hellier, P. F. L. Maxted, G. R. M. Miller, D. Pollacco, D. Queloz, E. Simpson, B. Smalley, A. H. M. J. Triaud, I. Boisse, F. Bouchy, M. Gillon, and G. Hébrard, Rossiter–McLaughlin effect measurements for WASP-16, WASP-25 and WASP-31*, Monthly Notices of the Royal Astronomical Society **423**, 1503 (2012).

[7] D. Fabrycky and S. Tremaine, Shrinking Binary and Planetary Orbits by Kozai Cycles with Tidal Friction, The Astrophysical Journal **669**, 1298 (2007).

[8] Y. Ohta, A. Taruya, and Y. Suto, The Rossiter-McLaughlin Effect and Analytic Radial Velocity Curves for Transiting Extrasolar Planetary Systems, The Astrophysical Journal **622**, 1118 (2005).

[9] B. S. Gaudi and J. N. Winn, Prospects for the Characterization and Confirmation of Transiting Exoplanets via the Rossiter-McLaughlin Effect, Astrophys. J. **655**, 550 (2007), arXiv:astro-ph/0608071 [astro-ph].

[10] R. A. Rossiter, On the detection of an effect of rotation during eclipse in the velocity of the brigher component of beta Lyrae, and on the constancy of velocity of this system., The Astrophysical Journal **60**, 15 (1924).

[11] D. B. McLaughlin, Some results of a spectrographic study of the Algol system., The Astrophysical Journal **60**, 22 (1924).

[12] R. P. Butler, J. T. Wright, G. W. Marcy, D. A. Fischer, S. S. Vogt, C. G. Tinney, H. R. A. Jones, B. D. Carter, J. A. Johnson, C. McCarthy, and A. J. Penny, Catalog of Nearby Exoplanets, The Astrophysical Journal **646**, 505 (2006).

[13] Pepe, F., Mayor, M., Queloz, D., Benz, W., Bonfils, X., Bouchy, F., Lo Curto, G., Lovis, C., Mégevand, D., Moutou, C., Naef, D., Rupprecht, G., Santos, N. C., Sivan, J.-P., Sosnowska, D., and Udry, S., The HARPS search for southern extra-solar planets* - I. HD075A new "hot Jupiter", A&A **423**, 385 (2004).

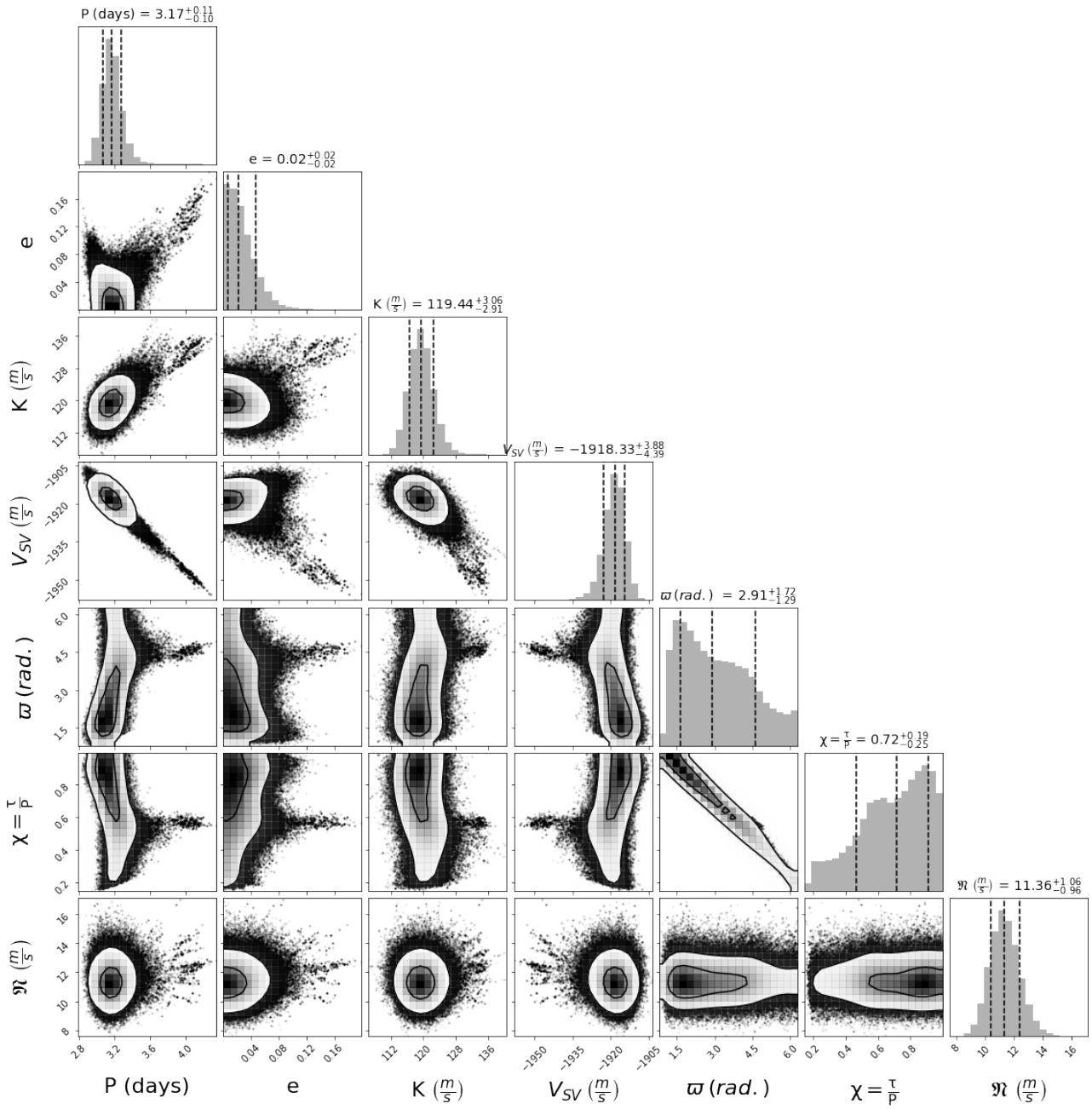

FIG. 6. Correlation of the orbital parameters of WASP-16 system. Here K is the semi-amplitude which is a function of m_p, m_s, n, a, and i. τ is the time of pericenter passage. The term $\mathfrak{N}$ accounts for any unknown measurement errors.